Position-Specific 13C Fractionation during Liquid–Vapor Transition Correlated to the Strength of Intermolecular Interaction in the Liquid Phase

Maxime Julien, Patrick Höhener, Richard J. Robins, Julien Parinet, Gérald S. Remaud

Position-Specific ^{13}C Fractionation during Liquid-Vapor Transition is Correlated to the Strength of Intermolecular Interaction in the Liquid Phase

Maxime Julien[1], Patrick Höhener[2], Richard J. Robins[1], Julien Parinet[2] and Gérald S. Remaud[1]*

[1] EBSI team, CEISAM, University of Nantes–CNRS UMR 6230, 2 rue de la Houssinière BP 92208, F-44322 Nantes, France.

[2] Laboratoire Chimie Environnement, University of Aix-Marseille–CNRS UMR 7376, place Victor Hugo 3, F-13331 Marseille, France.

Correspondence: G Remaud. Phone: 33 2 51 12 57 19; Fax: 33 2 51 12 57 12; e-mail: gerald.remaud@univ-nantes.fr

Abstract

The relationship between the strength of the intermolecular interaction in liquid and the position-specific ^{13}C fractionation observed during distillation was investigated. A range of molecules showing different intermolecular interactions in terms of mode and intensity were incorporated in the study. Although it had previously been suggested that during evaporation the diffusive ^{13}C isotope effect in the thin liquid layer interfaced with vapor is not position-specific, herein we show that this is not the case. In particular, the position-specific effect was demonstrated for a series of alcohols. Our hypothesis is that intermolecular interactions in the liquid phase are the source of position-specific ^{13}C fractionation observed on the molecule. A clear trend is observed between the ^{13}C isotope effect of the carbon bearing the heteroatom of chemical function and the relative permittivity, the solvent hydrogen-bond acidity and the solvent hydrogen-bond basicity, while only a weak trend was observed when using the ^{13}C content of the whole molecule. Furthermore two families of products appeared when using the hydrogen-bond acidity parameter for the correlation by distinguishing H-acceptors and H-donors molecules to those H-acceptors only. This strongly reinforces the hypothesis of an important role of the ^{13}C positioned close to the interaction center.

Keywords

Position-specific isotope fractionation; isotope ratio monitoring ^{13}C NMR spectrometry; Volatilization, Distillation, Craig-Gordon model

Introduction

Stable isotopes were widely used in the past to study the nature of phase transfer processes like liquid-vapor transfer (References Jancso and van Hook, book of Wolfberg et al, etc.). [12] Past studies used fully substituted isotopic molecules for which large isotope effects are observed which could be better measured with past analytical techniques. Progress in analytical techniques has led to the development of Compound-Specific Isotope Analysis (CSIA) capable of monitoring stable isotope ratios at natural abundance ratios. With the help of CSIA, the mechanisms of phase transfer processes were furthermore investigated and elucidated (Hunkeler and Jeannottat, Kuder, Huang, etc.). However, it has been shown that CSIA based on isotope ratio monitoring by Mass Spectrometry (irm-MS) is not always sufficient to describe the ^{13}C fractionation during the whole evaporation phenomenon. Recently, we have reported the study of several liquid-vapor transition processes using isotope ratio monitoring by ^{13}C Nuclear Magnetic Resonance spectrometry (irm-^{13}C NMR) in order to simulate position-specific fractionation during evaporation.[3] We have shown that Position-Specific Isotope Analysis (PSIA) by irm-^{13}C NMR can provide new insights into physical processes, including in circumstances in which CSIA may not detect any effect on the whole molecule.[4] Furthermore, bulk ^{13}C composition ($\delta^{13}C_{bulk}$) analysis (CSIA), obtained by irm-MS, only indicates which isotopologue reacts preferentially in the studied process, whereas PSIA shows which isotopomer is the most sensitive (see Figure 1 for a further definition).

Isotope fractionation is conveniently described by the isotopic fractionation factor α or the isotope effect IE and is associated with discrimination between the behavior of isotopomers.[5] A previous study showed that the Craig-Gordon isotope model, originally derived for water evaporation,[6] is also valid for organic liquids as demonstrated by Kuder and collaborators,[7]

especially for the description of the volatilization of nonpolar organic liquids with air-side limitation of the volatilization rate.[4] In the Craig-Gordon model in its original form, it is assumed that the diffusive effect in the stagnant liquid $\varepsilon_{diff\text{-}liq}$ (thin liquid layer interfaced with vapor, see ref 4) is not position-specific, i.e. is independent of the position of the ^{13}C in the molecule. However, among the compounds studied, ethanol and propan-1-ol both showed a position-specific behavior. Working with the hypothesis that intermolecular interactions in the liquid phase were the source of position-specific ^{13}C fractionation observed on the molecule collected from the vapor phase, we have therefore generated a modified Craig-Gordon equation to take these position-specific interactions into account.[4]

The most widespread non-covalent molecular interaction is hydrogen bonding. The strength of the hydrogen bond depends on the properties of both the hydrogen-bond acceptor (HBA) and the hydrogen-bond donor (HBD).[8] Recently, a specific methodology has been proposed by which both solvent hydrogen-bond basicity and solvent hydrogen-bond acidity can be quantified, leading to the parameters β_1[9] and ET(30),[10] respectively. β_1 is linked to the original scale of Kamlet and Taft[11] but is specific for the solvent scales. Thus, the scale of solvent hydrogen-bond basicity was established by the method that compares the ^{19}F NMR chemical shift of 4-fluorophenol and 4-fluoroanisole in hydrogen-bond acceptor solvent. In addition to the empirical parameter describing the hydrogen-bond acidity α_1 (from Kamlet-Taft), the quantitative solvent polarity parameter ET(30) was introduced. This is based on the negative solvachromism of 2,6-diphenyl-4-(2,4,6-triphenylpyridinium-1-yl)phenolate (known as betaine 30).[12] Weaker interactions are encompassed under van der Waals, π-bonding[13] or halogen-bond[14] interactions that explain intermolecular associations between apolar molecules, molecules possessing an

aromatic-ring, or halogen-containing compounds. The unit accounting for these interactions is the relative permittivity,[15] previously known as the dielectric constant diE.[11]

The goal of the present work was to investigate the relationship between the strength of the intermolecular interaction in liquid and the position-specific ^{13}C fractionation observed during vaporization. We asked three fundamental questions: "Does the presence of ^{13}C in the molecule increase (or decrease) the interaction?", "Is this interaction stabilized in a specific ^{13}C isotopomer?", and "What is the influence of the proximity of ^{13}C to the interaction site?" To answer these questions conditions are required in which the isotope fractionation measured should reflect the transition liquid-vapor only with the influence on the liquid phase, but with no further isotope effect in the vapor phase. These conditions are essentially met in distillation in which no diffusive boundary layer is occurring when the compounds are boiling. Furthermore, this process is quick, simple, and known to induce significant isotope effects in ^{2}H and ^{13}C.[16] Hence, this allows insight into isotope effects occurring on the liquid side. To express the isotope effect during the liquid-vapor transition we used the nomenclature already proposed for such transformation.[16a] In the case of a small transformation of the substrate, such as the collection of a very small distillate volume ($\leq 3\%$), any associated isotope effects can readily be detected in the distillate, but impact negligibly on the isotopomer composition of the remaining liquid. The corresponding fractionation factor α was defined in the classical literature as separation factor α (Jancso and Van Hook, 1974):

$$\alpha = (N'/N)_{vap}/(N'/N)_{liq} \quad (1)$$

where N' and N are the mole fractions of light and heavy isotopomers respectively in the system at equilibrium. The specific-isotope fractionation of site i (the isotopomer with ^{13}C at position isotopomer i) is then defined as the experimental fractionation factor α_{exp}:

$$\alpha_{exp,\,i} = (^{13}C/^{12}C)_{i,\,vap}/(^{13}C/^{12}C)_{i,\,liq} \quad (2)$$

Equation 2 is adapted to more recent work on stable isotopes where ratios are measured and expressed as abundance of heavy isotopes divided by abundance of light isotopes (Aelion et al, 2010). Thus, a normal isotope effect leads to $\alpha_{exp}<1$: i.e. the liquid (distillate) is impoverished in heavy isotopes with respect to the vapor (starting product), while an inverse isotope effect favoring the heavy atom in the vapor gives $\alpha_{exp}>1$. This is the convention that is used in the present work. Several compounds were selected with respect to their physicochemical properties in terms of hydrogen-bond capabilities, or more generally their intermolecular interactions. The code of the samples used and the carbon numbering are shown in Table 1. The alcohols are clearly hydrogen-bond acceptors and donors (amphiprotic solvents). Other chemical functions, such as those which involve heteroatoms, could be polar and/or hydrogen-bond acceptors. Furthermore, Br and Cl atoms may generate a halogen-bond. Two apolar compounds, toluene and *n*-heptane were also distilled for comparison. All the experiments were conducted at natural abundance isotope composition.

Experimental

Chemicals

Methyl *tert*-butyl ether (99.8%), *n*-heptane (99%), toluene (99.9%), bromoethane (98%), trichloroethylene (99.5%), propan-1-ol (99.7%), propan-2-ol (99%), butan-1-ol (99.7%), *tert*-butanol (99.5%), 2-methyl-2-butanol (99%), pentan-1-ol (99%), cyclohexanol (99%), ethyl acetate (99.9%), acetonitrile (99.9%), and 4-heptanone (98%), were obtained from Sigma-Aldrich. Ethanol (99.8%), methanol (98%) and chloroform (98%) were purchased from VWR

Prolabo and acetone (99.5%) from Alfa Aesar. DMSO-d_6, dioxane-d_8 and CD_3CN were obtained from Eurisotop. Tris(2,4-pentadionato)chromium(III) [$Cr(Acac)_3$] was from Merck.

Distillation experiments

For each experiment, 100 mL of pure compound was introduced into a 1 L round bottom flask and distillation was carried out using a Cadiot distillation column equipped with a Teflon spinning band (see Murray and reference therein for its characteristics[17]). This distillation equipment allows the reflux to be rigorously controlled. Once reflux conditions were reached, the distillate was collected up to approximately 3% maximum of the mass of the starting substrate. The distillate was then submitted to ^{13}C-irm-EA/MS and irm-^{13}C NMR.

In the present study, distillation has been chosen in order to study liquid-vapor equilibrium effects, because this method is quick and easy to perform which is perfect to study a large panel of chemical compounds in very controlled conditions. The inconvenient of this protocol is that the resulting isotope effects are magnified, especially using a spinning band distillation column which displays many theoretical plates and the capability of maintaining the system at equilibrium. Nevertheless, these overexpressed isotopic fractionations have the same direction (normal or inverse) as those observed in static phase equilibrium (Refs. Jeannottat+Hunkeler) or vapor pressure measurements (Jancso+Van Hook, 1974).

In the case of isotopic studies, the concept of “pure compound” needs to be further defined. The term “pure” means that there is only one chemical species present. However, it is in fact a mixture of all potential isotopologues and isotopomers of the considered compound. As an example, a sample of pure ethanol contains four types of molecules isotopically different in ^{13}C (see Figure 1).

^{13}C -irm-EA/MS

Bulk ^{13}C abundance ($\delta^{13}C_{bulk}$) was determined by irm-MS using an Integra2 spectrometer (Sercon Instruments, Crewe, UK) linked to a Sercon elemental analyser (EA) (Sercon Instruments, Crewe, UK). A precise amount of each compound was weighted into tin capsules (2x5 mm, Thermo Fisher scientific) using a 10^{-6} g precision balance (Ohaus Discovery DV215CD) to give approx. 0.4 mg of carbon for each compound. Great care was taken to ensure that there was no leakage from the capsule. First, during the weighing of the Volatile Organic Compound (VOC) introduced into the tin-capsule, the sealed capsule was left on the balance for a short delay to verify the stability of the mass. No change in mass indicated that the capsule was effectively sealed. Secondly, the percentage of carbon was checked by the operator by comparing this value with that usually obtained on the solid working reference. This gives a check in relation to the intensity of the signal of the ions obtained from the CO_2 generated from the different isotopologues (*m/z* = 44, 45, 46). Moreover, each sample is analyzed three times to ensure measuring true $\delta^{13}C$ values and a repeatability study has also been performed in a previous study (see ref 3) which demonstrates the capability of these experimental conditions to measure the bulk isotopic composition of VOCs such as MTBE. The $\delta^{13}C$ (‰) values were expressed relative to the international reference (Vienna-Pee Dee Belemnite, V-PDB) using the relationship: $\delta^{13}C_{VPDB}(‰) = \left(\frac{R_{sample}}{R_{standard}} - 1\right) \times 1000$.[18] The instrument was calibrated for $\delta^{13}C$ using the international reference materials NBS-22 ($\delta^{13}C_{PDB}$ = -30.03 ‰), SUCROSE-C6 ($\delta^{13}C_{PDB}$ = -10.80 ‰), and IAEA-CH-7 PEF-1 ($\delta^{13}C_{PDB}$ = -32.15 ‰) (IAEA, Vienna, Austria) and instrumental deviation followed via a laboratory working standard of glutamic acid.

Isotope ratio monitoring ^{13}C NMR spectrometry (irm-^{13}C NMR)

The sample preparation consisted of the successive addition in a 4 mL vial of the compound, the lock substance and the relaxation agent $Cr(Acac)_3$ (which acts to decrease the longitudinal relaxation time T1).[19] The respective amount of each was adapted according to (i) the T_1 values of the analyte, (ii) the reciprocal solubility with the deuterated solvents and/or the relaxation agent and (iii) the ^{13}C NMR spectrum: no peak overlapping. The exact preparation procedures were described previously.[3] Quantitative ^{13}C NMR spectra were recorded using an AVANCE I 400 spectrometer (Bruker Biospin, Wissembourg, France), fitted with a 5 mm i.d. $^{1}H/^{13}C$ dual^{+} probe, carefully tuned at the recording frequency of 100.61 MHz, or a Bruker AVANCE III 400 spectrometer fitted with a 5 mm i.d. BBFO probe tuned at the recording frequency of 100.62 MHz. The temperature of the probe was set to 303 K. Spectra were acquired without tube rotation. Isotope $^{13}C/^{12}C$ ratios were calculated from processed spectra as described previously.[3, 20]

Calculation of $\mathcal{E}_{bulk}$ and $\mathcal{E}_i$

The isotope effect IE (‰) was obtained from the equation:

$$IE = (\alpha_{=} - 1) \times 1000 \qquad (3)$$

where the isotope isotope effect (IE) is calculated as explained in detail in the work of Julien *et al.*[4] where IE is equivalent to ε.

Here IE<0 is a normal isotope effect is observed while IE>0 indicates an inverse isotope effect.

Results and discussion

Position-specific ^{13}C analysis by NMR

PSIA may be performed by fragmenting the molecule in such a way that, after subsequent analysis of the resulting fragments by irm-MS,[21] information on the isotopomer composition is retrieved. This fragmentation can conveniently be achieved on-line by pyrolysis prior to mass spectrometry analysis.[22] However, this approach is not easily applicable to molecules containing more than 4 carbon atoms. In contrast, quantitative NMR gives access to all spectrally-resolved sites in the compound, i.e. relative titration of the ^{13}C isotopomers constituting the molecule when irm-^{13}C NMR conditions are used.[23] It offers the advantage of directly analyzing the target molecule, hence avoiding the risk of technique-associated fractionation. The precision in irm-NMR depends primarily on the signal-to-noise ratio (SNR) and it is described in the present work by a standard deviation of 0.3‰ on the $\delta^{13}C$ scale (‰). We have shown in a previous study that, under these conditions, the uncertainty on IE_i is ±0.2‰ (95% confidence level)[24] for the evaporation processes and the molecules used.[3] This value is the threshold of significance that will be used for the interpretation of the results presented.

Bulk ^{13}C and position-specific fractionation upon distillation

Zhang *et al.* showed that distillation can be a useful tool to determine isotopic fractionation factors at equilibrium during liquid-vapor transitions.[16a] For a given compound heated at reflux, an equilibrium between the liquid and the vapor is established. When a very small amount of distillate is collected (≤ 3%) it can be assumed that the isotope profile of the distillate represents the isotopic composition of the vapor at equilibrium with the liquid. These authors measured ^{2}H the position-specific isotope effect (by irm-^{2}H NMR) as well as isotope bulk effect (by irm-MS) on heteroatoms (^{13}C, ^{15}N and ^{18}O) in a series of organic molecules containing typical functional groups. They observed that the isotopic fractionation enrichments varied with (i) the element, (ii)

the type of chemical function and (iii) the ^{2}H isotopomers (^{2}H position in the molecule). We previously confirmed that distillation under similar conditions also led to position-specific ^{13}C fractionation in ethanol: the distillate is enriched in ^{13}C mainly on the CH_2 moiety.[3, 16b] In the present work we have extended this protocol to other organic compounds that have several specific chemical characteristics in terms of substituent, heteroatoms and chemical functions. The isotopomer profiles expressed as $\delta^{13}C_{bulk}$, $\delta^{13}C_i$ and $\Delta\delta^{13}C$ (difference between the $\delta^{13}C$ in distillate and $\delta^{13}C$ in starting material) are summarized in Table 2. Two key observations can be made. First, in the majority of cases the distillate is enriched in ^{13}C. Second, a large variability of $\Delta\delta^{13}C_i$ within and between molecules is seen. In a previous study (ref 4), ^{13}C isotopic fractionation associated with distillation has been determined analyzing the remaining substrate after distillation of 93 to 98% of pure compound. Under these conditions, it can be assumed that the detected isotopic fractionation corresponds to the isotope effect associated with the liquid-vapor transformation without contribution of the diffusion. In the present case, the distillate has been analyzed in order to study the isotopic fractionation associated with distillation. The low distillation yields (around 3%) along with the presence of multiple theoretical plates both induce the detection of larger isotope effects than the analysis of the remaining substrate. However, this overestimation of the isotopic fractionation associated with distillation is not misleading for the interpretation because the intramolecular distribution of the fractionation is conserved. As an example, the analysis of the distillation tail of TCE showed an isotope effect of +0.8‰ mostly located on the carbon bearing two chlorine atoms (see ref 4) and this isotope effects is about +5.1‰ in the present study but still mostly located on the same carbon position (see Table 3). The distillation protocol employed in this study doesn't allow obtaining true values of liquid-vapor equilibrium isotope effect but it is still available to study its mechanism. Table 1 shows the

numbering of the carbon positions, according to the shielding order of the peak in the ^{13}C NMR spectrum. This shielding (or deshielding) is associated with the electron density surrounding the given carbon atom and depends to some degree on the polarity of the neighboring heteroatoms (or chemical functions). The isotopomer 'C-1' which contains the ^{13}C directly linked to this heteroatom is clearly identified in alcohols. It is, however, less straightforward for other chemical species, such as ester, ketone, nitrile, etc. (see Table 1 for the attribution of C-1 in each molecule). In general, the ^{13}C ratio at the C-1 is seen to be the most effected by the liquid-vapor transition, i.e. it is the isotopomer containing ^{13}C at that position which distils first. Exceptions are notable for acetonitrile (acni), for which $\delta^{13}C_{C\text{-}1}$ is depleted, and for *n*-heptane (hept) and toluene (tol) for which there is a homogeneous enrichment effect for each carbon. In the series of alcohols, a further effect is observed: the preference of the ^{13}C isotopomer for the vapor phase is diminished, stabilized or even increased according to the distance from the OH function along the carbon chain. Thus, in butan-1-ol (al-5) and pentan-1-ol (al-8) $\Delta\delta^{13}C$ upon distillation is large for the carbon-bearing OH (C-1): +5‰ and +4.1‰, lower for the inner carbon(s) of the chain: +3.0/+2.6‰ and +2.7/+2.0‰ and slightly larger for the terminal carbon positions: +2.9 and +2.7‰ respectively (Table 2). This is clear evidence that the presence of ^{13}C close to the OH function influences strongly the facility for the molecule to be transformed into vapor. Interestingly, a remote effect is associated with the terminal carbon.

Position-specific ^{13}C fractionation versus intermolecular interactions

The above discussion of the alcohol series addresses the issue of interactions within the liquid. As a first deduction, it appears that the proximity of ^{13}C to the OH function favors the distillation of the corresponding isotopomer. Therefore the question is: does $\varepsilon_{C\text{-}1}$ (the amplitude of the ^{13}C

fractionation or the discrimination between the isotopomer C-1 and the other isotopomers) represent the strength of the interaction between alcohol molecules in the liquid state? Among several parameters used for describing the potential level of intermolecular associations, the relative permittivity (diE) is the most commonly used. Table 3 reports the isotope effects (IE_{bulk} and IE_{C-1}), diE, ET(30) and β1 (see Introduction for a definition of these terms). Unfortunately, these parameters are not available in the literature for all the molecules studied, but sufficient values are available to establish trend lines. These lines have been drawn according to the visual distribution of data points, which means that Figures 2 and 3 do not present real correlations between isotope effects and the physical properties of compounds but, rather, lines drawn without *a priori* to make the discussion easier. Trend lines have been drawn using Microsoft Excel so they have an equation and a root mean square (R^2) which also are detailed in Figures captions in order to help the discussion the results. Figures 2 and 3 illustrate the potential trends between the isotope effects and diE, ET(30) and β1, respectively. A clear trend is observed between IE_{C-1} and diE, ET(30) and a weaker for β1 (Figures 2), while a loose trend can even be discerned between IE_{bulk} and diE, ET(30) and β1 (Figures 3). This strongly reinforces the deduction of an important role of the ^{13}C isotopomer C-1 in the interaction between molecules.

Nevertheless, there are some exceptions which deserve comment. In all cases, toluene (tol) and even more so *n*-heptane (hept) do not follow these trends: this is readily explained by the lack of polarity (no diE) and an inability to form H-bonds or, more generally, interactions involving a specific position in the molecule. Both *n*-heptane and toluene are only able to form van der Waals and π bonding interactions, respectively, that do not induce any significant position-specific isotope effect during distillation. Interestingly, the data for bromoethane (brom) do not fit with the β1 values either (Figure 2c) when it appears to have a behavior similar to alcohols concerning

ET(30) trends (Figure 2b). Since the parameters β1 and ET(30) describe the potential interaction of the molecule as a solvent,[9] it can be seen here that the molecule acts both as solute and solvent, i.e. in a self-association. Therefore, a molecule may be in a state to give or to receive H (or another interaction) but not to do both at the same time. Thus bromoethane shows a weak base-property, with a halogen-type association likely to be occurring.

As can be seen from Figure 2b, a clear double trend is observed. One encompasses the alcohols (al-x), but also chloroform (chlo), which are both H-acceptors and H-donors (a proton can readily be exchanged with deuterium[25]), and to some extent bromoethane (brom). The case of chloroform, with the isotope effect associated with its distillation correlating very well with those for alcohols (See Figure 2b), is interesting. This could be explained by (i) the high electron density in this molecule and (ii) the resulting presence of the acidic hydrogen. These two features of chloroform can interact forming a halogen bond and its strength seems to be dependent of the presence of a ^{13}C on the central carbon position. Trichloroethene (TCE) presents an isotope effect mostly located on the carbon bearing the acidic hydrogen that can form hydrogen bonds, but this compound better correlates with H-acceptors (Figure 2b). Of the remaining products studied, that are H-acceptors only, acetonitrile (acni), acetone (acet) and ethyl acetate (etac) all show good correlation with amphiprotic molecules (alcohols) (Figures 2 and 3).

A change in the solvation shell of ethanol modifies the ^{13}C position-specific fractionation. As an illustration, the distillation of a dilute acidic aqueous ethanol solution (10% v/v with 1 M H_2SO_4), using the same device, leads to the following isotope effect IE, measured on the distillate: bulk, +3.4‰, C-1, +6.3‰, C-2, +0.5‰. By increasing the H-bond network around the ethanol molecule, the $\varepsilon_{C\text{-}1}$ is accentuated, thus confirming that the isotopomer containing a ^{12}C at the C-1 position reinforces the intermolecular interaction. Interestingly, the reverse is found for the

position C-2 for which it is the isotopomer with a ^{12}C on the CH_3 that distils first. The significance of such behaviors is beyond the scope of this paper, but it is clear that the ^{13}C position-specific fractionation is sensitive to the types of interaction and to the models of association: most probably a large network (complex) for alcohols and chloroform versus a binary association (simple) for the other compounds investigated.

Conclusion

The main outcomes of this study are two-fold. First, it is shown that position-specific fractionation in liquid-vapor transitions can occur in a range of molecules. When the molecular architecture within the liquid enables interactions, then the isotope effect of diffusion $\varepsilon_{diff\text{-}liq}$ (ref 4) is position-specific. This is a novel finding, since up to now it has been considered that ^{13}C fractionation during diffusion shows a mass effect only, i.e. is not position-specific. These new data now need to be included in the model of fractionation during the process of volatilization according to the Craig-Gordon isotope model for organic liquids.[4, 7] Second, ^{13}C position-specific fractionation appears to be exploitable as a marker of the strength of interactions in the liquid phase within the self-association framework. Fundamentally, the presence of a ^{13}C atom in a molecule according to its position decreases the interaction strength. How the presence of a ^{13}C acts to (de)stabilize the H-bond in alcohols now needs to be further investigated by theoretical modelling. Other intermolecular interactions such as the dimerization of carboxylic acids could also be studied using the same approach. Moreover, more complex systems such as VOCs diffusive transport in soil could be studied in the same way where the presence of heavy carbon isotopes should also have an influence on isotopic fractionation associated with diffusion.

Acknowledgments

This work is funded by the French National Research Agency (ANR), project ISOTO-POL in the program CESA (N° 009 01). M. Julien thanks the Région Pays de la Loire for funding his postdoctoral bursary through the project PLAISIR. We thank Ms. Anne-Marie Schiphorst for help with irm-MS measurements and Jérôme Graton and Jean-Yves Lequestel for fruitful discussions on inter-molecular interactions.

References

1. Hofstetter, T. B.; Berg, M., Assessing transformation processes of organic contaminants by compound-specific stable isotope analysis. *Trends Anal. Chem.* **2011,** *30*, 618-627.
2. (a) Elsner, M.; Jochmann, M. A.; Hofstetter, T. B.; Hunkeler, D.; Bernstein, A.; Schmidt, T. C.; Schimmelmann, A., Current challenges in compound-specific stable isotope analysis of environmental organic contaminants. *Anal. Bioanal. Chem.* **2012,** *403*, 2471-91; (b) Thullner, M.; Centler, F.; Richnow, H.-H.; Fischer, A., Quantification of organic pollutant degradation in contaminated aquifers using compound specific stable isotope analysis – Review of recent developments. *Org. Geochem.* **2012,** *42*, 1440-1460.
3. Julien, M.; Parinet, J.; Nun, P.; Bayle, K.; Höhener, P.; Robins, R. J.; Remaud, G. S., Fractionation in position-specific isotope composition during vaporization of environmental pollutants measured with isotope ratio monitoring by ^{13}C nuclear magnetic resonance spectrometry. *Environ. Pollut.* **2015,** *205*, 299-306.
4. Julien, M.; Nun, P.; Robins, R. J.; Remaud, G. S.; Parinet, J.; Höhener, P., Insights into Mechanistic Models for Evaporation of Organic Liquids in the Environment Obtained by Position-Specific Carbon Isotope Analysis. *Environ. Sci. Technol.* **2015,** *49*, 12782-12788.

5. Jeannottat, S.; Hunkeler, D., Chlorine and Carbon Isotopes Fractionation during Volatilization and Diffusive Transport of Trichloroethene in the Unsaturated Zone. *Environ. Sci. Technol.* **2012,** *46*, 3169-3176.

6. Craig, H.; Gordon, L. I., Deuterium and oxygen 18 variations in the ocean and the marine atmosphere. In *Conference on Stable Isotopes in Oceanographic Studies and Paleotemperatures*, Spoleto, Italy, 1965; Vol. 9.

7. Kuder, T.; Philp, P.; Allen, J., Effects of volatilization on carbon and hydrogen isotope ratios of MTBE. *Environ. Sci. Technol.* **2009,** *43*, 1763-8.

8. Laurence, C.; Brameld, K. A.; Graton, J.; Le Questel, J.-Y.; Renault, E., The pKBHX Database: Toward a Better Understanding of Hydrogen-Bond Basicity for Medicinal Chemists. *J. Med. Chem.* **2009,** *52*, 4073-4086.

9. Laurence, C.; Legros, J.; Nicolet, P.; Vuluga, D.; Chantzis, A.; Jacquemin, D., Solvatomagnetic Comparison Method: A Proper Quantification of Solvent Hydrogen-Bond Basicity. *J. Phys. Chem. B* **2014,** *118*, 7594-7608.

10. (a) Cerón-Carrasco, J. P.; Jacquemin, D.; Laurence, C.; Planchat, A.; Reichardt, C.; Sraïdi, K., Solvent polarity scales: determination of new ET(30) values for 84 organic solvents. *J. Phys. Org. Chem.* **2014,** *27*, 512-518; (b) Cerón-Carrasco, J. P.; Jacquemin, D.; Laurence, C.; Planchat, A.; Reichardt, C.; Sraïdi, K., Determination of a Solvent Hydrogen-Bond Acidity Scale by Means of the Solvatochromism of Pyridinium-N-phenolate Betaine Dye 30 and PCM-TD-DFT Calculations. *J. Phys. Chem. B* **2014,** *118*, 4605-4614.

11. Barwick, V. J., Strategies for solvent selection — a literature review. *Trends Anal. Chem.* **1997,** *16*, 293-309.

12. (a) Reichardt, C., Solvatochromism, thermochromism, piezochromism, halochromism, and chiro-solvatochromism of pyridinium N-phenoxide betaine dyes. *Chem. Soc. Rev.* **1992,** *21*,

147-153; (b) Reichardt, C., Solvatochromic Dyes as Solvent Polarity Indicators. *Chem. Rev.* **1994,** *94*, 2319-2358.

13. Meyer, E. A.; Castellano, R. K.; Diederich, F., Interactions with Aromatic Rings in Chemical and Biological Recognition. *Angew. Chem. Int. Ed.* **2003,** *42*, 1210-1250.

14. Politzer, P.; Lane, P.; Concha, M. C.; Ma, Y.; Murray, J. S., An overview of halogen bonding. *J. Mol. Model.* **2007,** *13*, 305-311.

15. Braslavsky, S. E., Glossary of terms used in photochemistry, 3rd edition (IUPAC Recommendations 2006). *Pure Appl. Chem.* **2007,** *79*, 293-465.

16. (a) Zhang, B.-L.; Jouitteau, C.; Pionnier, S.; Gentil, E., Determination of Multiple Equilibrium Isotopic Fractionation Factors at Natural Abundance in Liquid-Vapor Transitions of Organic Molecules. *J. Phys. Chem. B* **2002,** *106*, 2983-2988; (b) Botosoa, E. P.; Caytan, E.; Silvestre, V.; Robins, R. J.; Akoka, S.; Remaud, G. S., Unexpected Fractionation in Site-Specific ^{13}C Isotopic Distribution Detected by Quantitative ^{13}C NMR at Natural Abundance. *J. Am. Chem. Soc.* **2008,** *130*, 414-415.

17. Murray, K. E., A modified spinning band column for low pressure fractionation. *J. Am. Oil Chem. Soc.* **1951,** *28*, 235-239.

18. Muccio, Z.; Jackson, G. P., Isotope ratio mass spectrometry. *Analyst* **2009,** *134*, 213-222.

19. Caytan, E.; Remaud, G. S.; Tenailleau, E.; Akoka, S., Precise and accurate quantitative ^{13}C NMR with reduced experimental time. *Talanta* **2007,** *71*, 1016-1021.

20. (a) Silvestre, V.; Mboula, V. M.; Jouitteau, C.; Akoka, S.; Robins, R. J.; Remaud, G. S., Isotopic ^{13}C NMR spectrometry to assess counterfeiting of active pharmaceutical ingredients: Site-specific ^{13}C content of aspirin and paracetamol. *J. Pharm. Biomed. Anal.* **2009,** *50*, 336-341; (b) Bayle, K.; Akoka, S.; Remaud, G. S.; Robins, R. J., Nonstatistical

^{13}C Distribution during Carbon Transfer from Glucose to Ethanol during Fermentation Is Determined by the Catabolic Pathway Exploited. *J. Biol. Chem.* **2015,** *290*, 4118-4128.

21. (a) Meinschein, W. G.; Rinaldi, G. G. L.; Hayes, J. M.; Schoeller, D. A., Intramolecular isotopic order in biologically produced acetic acid. *Biol. Mass Spectrom.* **1974,** *1*, 172-174; (b) Rinaldi, G.; Meinschein, W. G.; Hayes, J. M., Intramolecular carbon isotopic distribution in biologically produced acetoin. *Biol. Mass Spectrom.* **1974,** *1*, 415-417; (c) Monson, K. D.; Hayes, J. M., Carbon isotopic fractionation in the biosynthesis of bacterial fatty acids. Ozonolysis of unsaturated fatty acids as a means of determining the intramolecular distribution of carbon isotopes. *Geochim. Cosmochim. Acta* **1982,** *46*, 139-149; (d) Weilacher, T.; Gleixner, G.; Schmidt, H.-L., Carbon isotope pattern in purine alkaloids a key to isotope discriminations in C1 compounds. *Phytochemistry* **1996,** *41*, 1073-1077.

22. (a) Corso, T. N.; Brenna, J. T., High-precision position-specific isotope analysis. *Proc. Natl. Acad. Sci. USA* **1997,** *94*, 1049-1053; (b) Dias, R. F.; Freeman, K. H.; Franks, S. G., Gas chromatography–pyrolysis–isotope ratio mass spectrometry: a new method for investigating intramolecular isotopic variation in low molecular weight organic acids. *Org. Geochem.* **2002,** *33*, 161-168; (c) Yamada, K.; Tanaka, M.; Nakagawa, F.; Yoshida, N., On-line measurement of intramolecular carbon isotope distribution of acetic acid by continuous-flow isotope ratio mass spectrometry. *Rapid Commun. Mass Spectrom.* **2002,** *16*, 1059-64; (d) Hattori, R.; Yamada, K.; Kikuchi, M.; Hirano, S.; Yoshida, N., Intramolecular carbon isotope distribution of acetic acid in vinegar. *J. Agric. Food. Chem.* **2011,** *59*, 9049-53; (e) Gauchotte, C.; O'Sullivan, G.; Davis, S.; Kalin, R. M., Development of an advanced on-line position-specific stable carbon isotope system and application to methyl tert-butyl ether. *Rapid Commun. Mass Spectrom.* **2009,** *23*, 3183-93; (f) Gilbert, A.;

Hattori, R.; Silvestre, V.; Wasano, N.; Akoka, S.; Hirano, S.; Yamada, K.; Yoshida, N.; Remaud, G. S., Comparison of IRMS and NMR spectrometry for the determination of intramolecular ^{13}C isotope composition: Application to ethanol. *Talanta* **2012,** *99*, 1035-1039.

23. Bayle, K.; Gilbert, A.; Julien, M.; Yamada, K.; Silvestre, V.; Robins, R. J.; Akoka, S.; Yoshida, N.; Remaud, G. S., Conditions to obtain precise and true measurements of the intramolecular ^{13}C distribution in organic molecules by isotopic ^{13}C nuclear magnetic resonance spectrometry. *Anal. Chim. Acta* **2014,** *846*, 1-7.

24. JCGM/WG, Evaluation of measurement data- Guide to the expression of uncertainty in measurement. *Evaluation of measurement data- Guide to the expression of uncertainty in measurement* **2008,** *100*.

25. Iwasaki, M.; Sakka, T.; Ohashi, S.; Matsushita, H.; Yokoyama, A.; Suzuki, K., Hydrogen/deuterium exchange reaction between chloroform and water-d2 in two-liquid-phase system. *J. Phys. Chem.* **1989,** *93*, 5139-5143.

Figure Captions

Figure 1. Definition of isotopologues and isotopomers: example of ethanol.

Figure 2. Relationship between the isotope effect located on position C-1 (IE_{C-1}) and (a) the relative permittivity (diE), (b) the hydrogen bond acidity (ET(30)), y=-0.31x+19.89, R^2=0.853 for both H-acceptors and H-donors, y=-0.80x+34.69, R^2=0.938 for H-acceptors only and (c) the hydrogen bond basicity (β_1), y=16.1x-6.37, R^2=0.619.

Figure 3. Relationship between the bulk isotope effect (IE_{Bulk}) and (a) the relative permittivity (diE), (b) the hydrogen bond acidity (ET(30)) y=-0.20x+13.39, R^2=0.359 for both H-acceptors and H-donors, y=-0.36x+15.65, R^2=0.643 for H-acceptors only and (c) the hydrogen bond basicity (β_1).

Figures

Figure 1.

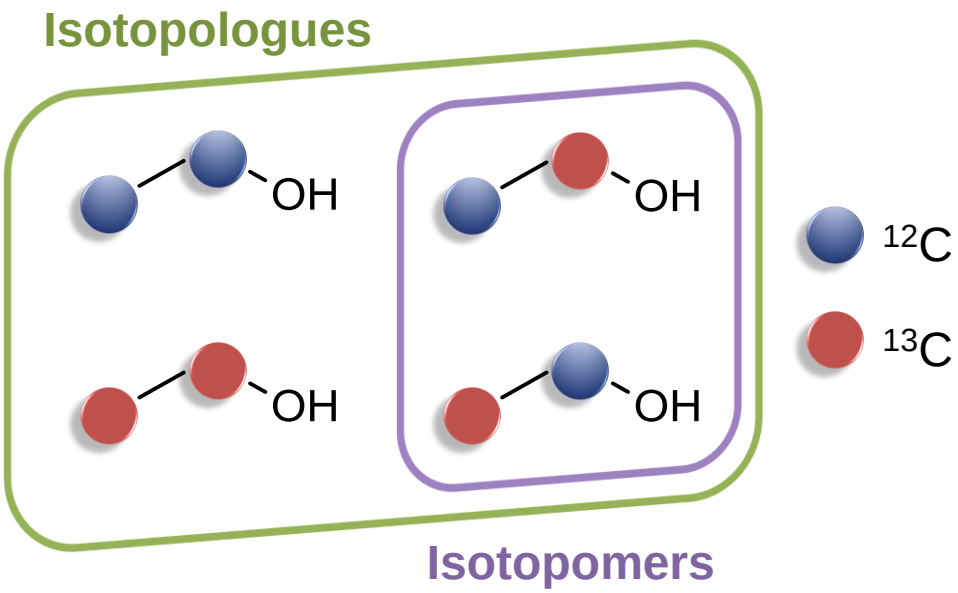

Figure 2.

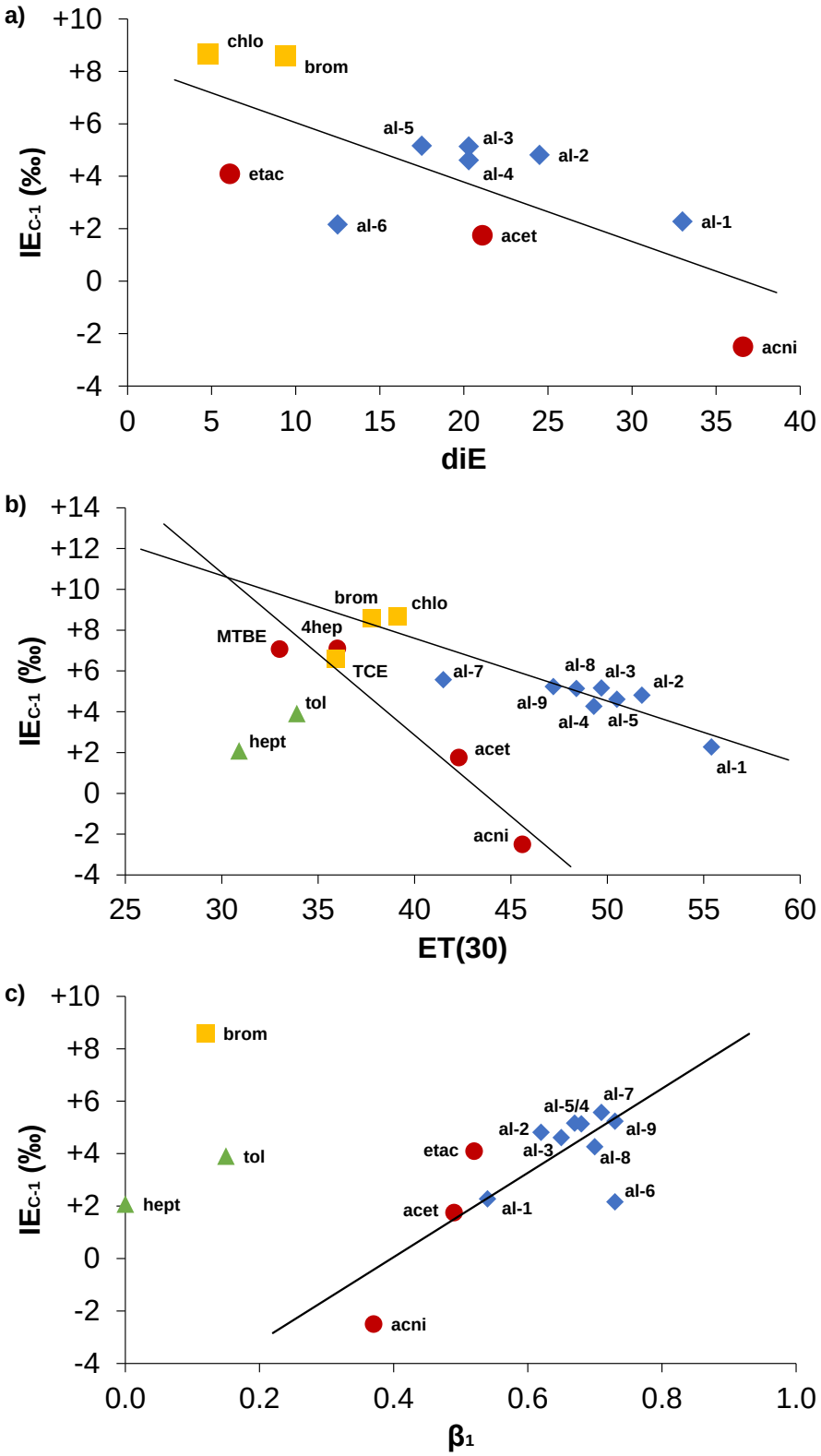
a)
IEC-1 (‰)
diE
chlo
brom
al-5
al-3
al-2
al-4
etac
al-6
acet
al-1
acni
b)
IEC-1 (‰)
ET(30)
brom
chlo
MTBE
4hep
TCE
al-7
al-8
al-3
al-2
al-9
al-4
al-5
tol
hept
acet
al-1
acni
c)
IEC-1 (‰)
β1
brom
al-5/4
al-7
al-2
al-9
al-3
etac
al-8
tol
al-6
hept
acet
al-1
acni

491 **Figure 3.**
492

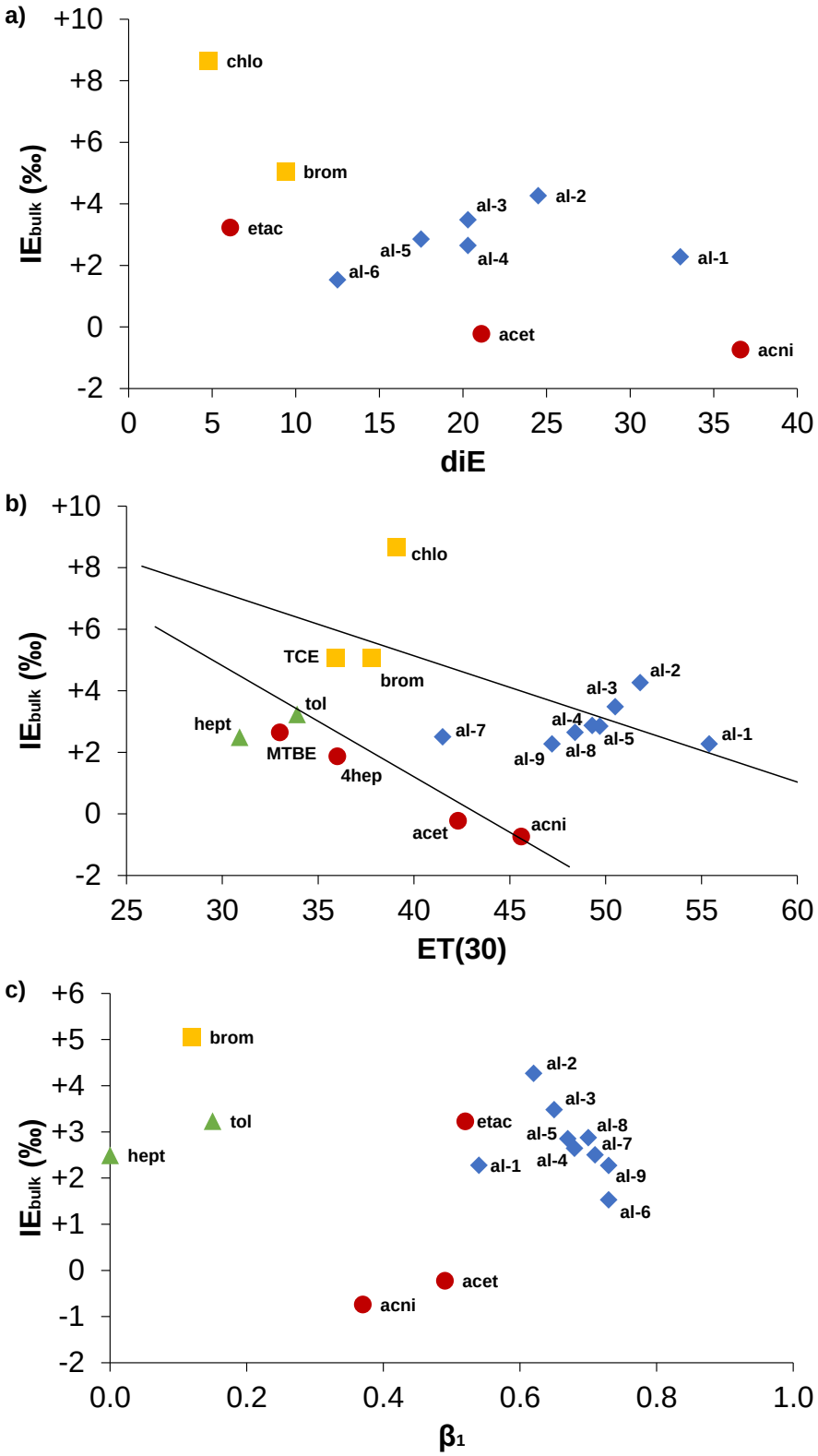

493

Table 1. Molecular structure of each compound investigated with the carbon atoms numbered in decreasing chemical shift in the ^{13}C NMR spectrum. The code of each sample used in Fig. 3 and 4 and in the Tables is also defined.

code	compound	structure
al-1	methanol	
al-2	ethanol	
al-3	propan-1-ol	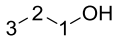
al-4	propan-2-ol	
al-5	butan-1-ol	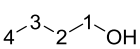
al-6	*tert*-butanol (TBA)	
al-7	2-methyl-2-butanol	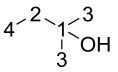
al-8	pentan-1-ol	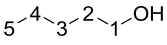
al-9	cyclohexanol	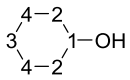
chlo	chloroform	
brom	bromoethane	
TCE	trichloroethylene	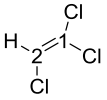
acet	acetone	
4hep	4-heptanone	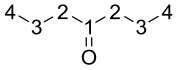
acni	acetonitrile	
etac	ethyl acetate	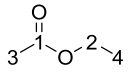
MTBE	MTBE	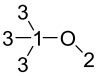
tol	toluene	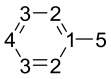
hept	*n*-heptane	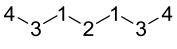

Table 2. ^{13}C isotope composition δ in ‰ and the difference between ^{13}C content of the starting material and of the distillate δΔ in ‰ for bulk isotopologue and each isotopomer of the studied samples (see Table 1 for denomination and carbon numbering).

Sample		Bulk	C-1	C-2	C-3	C-4	C-5
al-1	$\delta^{13}C$ initial	-30.7	-30.7				
	$\delta^{13}C$ distillate	-28.5	-28.5				
	$\Delta\delta^{13}C$	+2.2	+2.2				
al-2	$\delta^{13}C$ initial	-28.9	-32.2	-25.5			
	$\delta^{13}C$ distillate	-24.8	-27.5	-22.0			
	$\Delta\delta^{13}C$	+4.2	+4.7	+3.6			
al-3	$\delta^{13}C$ initial	-32.6	-35.5	-28.1	-34.1		
	$\delta^{13}C$ distillate	-29.2	-31.1	-25.1	-31.5		
	$\Delta\delta^{13}C$	+3.4	+4.5	+3.1	+2.6		
al-4	$\delta^{13}C$ initial	-26.9	-22.6	-29.1			
	$\delta^{13}C$ distillate	-24.4	-17.6	-27.7			
	$\Delta\delta^{13}C$	+2.6	+5.0	+1.3			
al-5	$\delta^{13}C$ initial	-31.0	-42.7	-29.1	-24.9	-28.5	
	$\delta^{13}C$ distillate	-28.3	-37.7	-26.1	-22.4	-25.6	
	$\Delta\delta^{13}C$	+2.8	+5.0	+3.0	+2.6	+2.9	
al-6	$\delta^{13}C$ initial	-25.4	-17.1	-28.2			
	$\delta^{13}C$ distillate	-23.9	-15.0	-26.9			
	$\Delta\delta^{13}C$	+1.5	+2.1	+1.3			
al-7	$\delta^{13}C$ initial	-31.2	-20.6	-28.0	-28.5	-50.5	
	$\delta^{13}C$ distillate	-28.8	-15.1	-26.3	-27.1	-48.3	
	$\Delta\delta^{13}C$	+2.4	+5.5	+1.7	+1.4	+2.1	
al-8	$\delta^{13}C$ initial	-28.3	-36.5	-23.9	-27.8	-26.2	-27.1
	$\delta^{13}C$ distillate	-25.5	-32.4	-21.3	-25.3	-24.2	-24.4
	$\Delta\delta^{13}C$	+2.8	+4.1	+2.6	+2.5	+2.0	+2.7
al-9	$\delta^{13}C$ initial	-24.4	-39.0	-17.2	-18.9	-26.9	
	$\delta^{13}C$ distillate	-22.2	-33.9	-17.8	-17.4	-23.0	
	$\Delta\delta^{13}C$	+2.2	+5.1	-0.5	+1.5	+3.9	
chlo	$\delta^{13}C$ initial	-41.7					
	$\delta^{13}C$ distillate	-33.4					
	$\Delta\delta^{13}C$	+8.4					

Table 2. (continued)

Sample		Bulk	C-1	C-2	C-3	C-4	C-5
brom	$\delta^{13}C$ initial	-11.6	-12.7	-10.4			
	$\delta^{13}C$ distillate	-6.6	-4.2	-9.0			
	$\Delta\delta^{13}C$	+5.0	+8.6	+1.5			
TCE	$\delta^{13}C$ initial	-29.6	-30.9	-28.3			
	$\delta^{13}C$ distillate	-24.6	-24.5	-24.8			
	$\Delta\delta^{13}C$	+4.9	+6.4	+3.5			
acet	$\delta^{13}C$ initial	-22.3	+8.8	-37.9			
	$\delta^{13}C$ distillate	-22.6	+10.6	-39.1			
	$\Delta\delta^{13}C$	-0.2	+1.8	-1.2			
4hep	$\delta^{13}C$ initial	-28.2	-23.5	-26.7	-29.0	-31.4	
	$\delta^{13}C$ distillate	-26.4	-16.5	-26.4	-27.5	-30.2	
	$\Delta\delta^{13}C$	+1.8	+7.0	+0.3	+1.4	+1.2	
acni	$\delta^{13}C$ initial	-24.5	-2.7	-46.3			
	$\delta^{13}C$ distillate	-25.2	-5.2	-45.3			
	$\Delta\delta^{13}C$	-0.7	-2.5	+1.0			
etac	$\delta^{13}C$ initial	-30.6	-19.5	-48.1	-30.7	-29.6	
	$\delta^{13}C$ distillate	-27.5	-15.5	-42.5	-31.0	-29.0	
	$\Delta\delta^{13}C$	+3.1	+4.0	+5.6	-0.3	+0.5	
MTBE	$\delta^{13}C$ initial	-28.6	-22.1	-39.3	-27.3		
	$\delta^{13}C$ distillate	-26.1	-15.1	-37.4	-25.9		
	$\Delta\delta^{13}C$	+2.6	+7.0	+1.8	+1.4		
tol	$\delta^{13}C$ initial	-22.8	-10.4	-23.3	-26.4	-26.1	-23.5
	$\delta^{13}C$ distillate	-19.6	-6.5	-21.1	-22.9	-22.6	-20.3
	$\Delta\delta^{13}C$	+3.2	+3.9	+2.2	+3.6	+3.6	+3.2
hept	$\delta^{13}C$ initial	-27.5	-25.3	-34.3	-26.3	-27.6	
	$\delta^{13}C$ distillate	-25.1	-23.2	-31.2	-24.0	-25.0	
	$\Delta\delta^{13}C$	+2.4	+2.0	+3.1	+2.3	+2.6	

509 **Table 3.** Isotope effect IE in ‰ for bulk and isotopomer C-1, relative permittivity (dielectric
510 constant) diE, solvent hydrogen-bond acidity ET(30) and hydrogen-bond basicity β_1 of the
511 studied samples (see Table 1 for denomination).

512

code	IE_{bulk}	IE_{C-1}	ET(30)	β_1	dielectric constant
al-1	+2.3	+2.3	55.4	0.54	33.0
al-2	+4.3	+4.8	51.8	0.62	24.5
al-3	+3.5	+4.6	50.5	0.65	20.3
al-4	+2.6	+5.1	48.4	0.68	20.3
al-5	+2.9	+5.2	49.7	0.67	17.5
al-6	+1.5	+2.2	nd	0.73	12.5
al-7	+2.5	+5.6	41.5	0.71	nd
al-8	+2.9	+4.3	49.3	0.70	nd
al-9	+2.3	+5.2	47.2	0.73	nd
chlo	+8.7	+8.7	39.1	nd	4.8
brom	+5.1	+8.6	37.8	0.12	9.4
TCE	+5.1	+6.6	35.9	nd	nd
acet	-0.2	+1.8	42.3	0.49	21.1
2hep	+1.3	-0.2	nd	nd	nd
3hep	+1.8	+1.1	nd	nd	nd
4hep	+1.9	+7.1	36.0	nd	nd
acni	-0.7	-2.5	45.6	0.37	36.6
etac	+3.2	+4.1	nd	0.52	6.1
MTBE	+2.6	+7.1	33.0	nd	nd
TAME	+3.5	+6.7	nd	nd	nd
tol	+3.2	+3.9	33.9	0.15	nd
hept	+2.5	+2.1	30.9	0.00	nd

513
514
515
516

517 **Table of Contents (TOC) graphic**

518

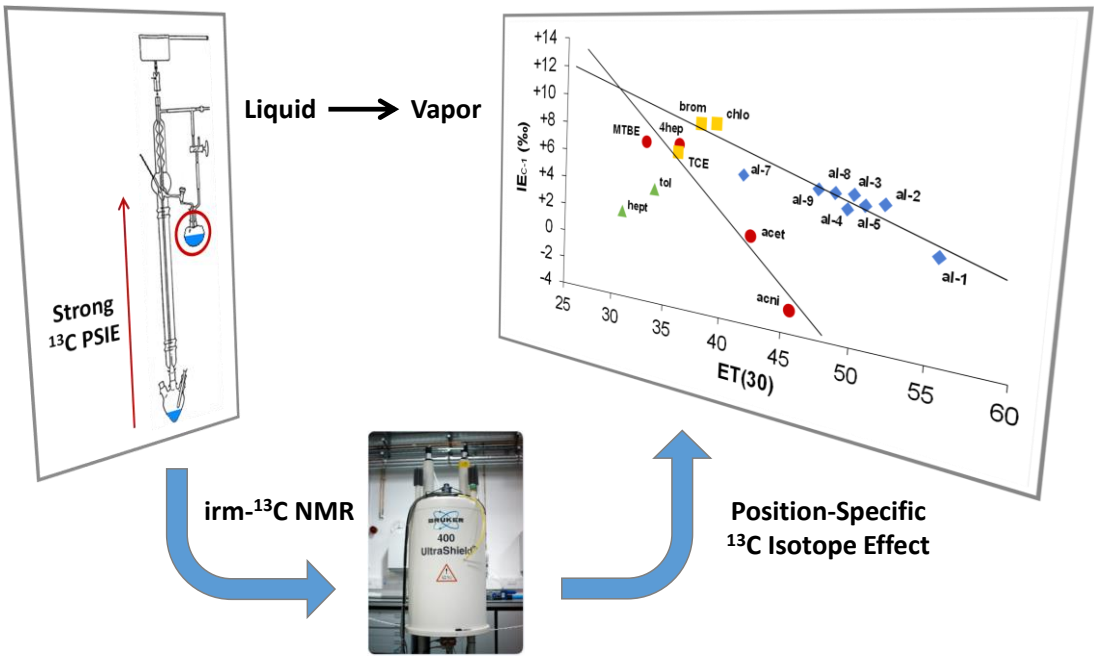

519